

# NATIONAL ADVISORY COMMITTEE FOR AERONAUTICS

## TECHNICAL NOTE

No. 1719

### FLIGHT MEASUREMENTS OF BUFFETING TAIL LOADS

By Allen R. Stokke and William S. Aiken, Jr.

Langley Aeronautical Laboratory  
Langley Field, Va.



Washington

October 1948

**Reproduced From  
Best Available Copy**

**20000807 167**

**DISTRIBUTION STATEMENT A**  
Approved for Public Release  
Distribution Unlimited

DTIC QUALITY INSPECTED 4

A9M00-113609

NATIONAL ADVISORY COMMITTEE FOR AERONAUTICS

TECHNICAL NOTE NO. 1719

FLIGHT MEASUREMENTS OF BUFFETING TAIL LOADS

By Allen R. Stokke and William S. Aiken, Jr.

SUMMARY

The magnitudes and frequencies of buffeting loads on the horizontal tail of a fighter-type airplane have been determined in flight for Mach numbers to about 0.80. Conditions of flight under which buffeting of the horizontal tail occurs have also been determined.

For the test airplane, buffeting of the horizontal tail occurred simultaneously with the attainment of maximum normal force at Mach numbers below about 0.64. Above this value of Mach number, buffeting occurred before the attainment of maximum normal force. In the range tested, Reynolds number had no appreciable effect on the buffeting boundary determined in abrupt pull-ups. The buffeting tail-load increment for constant dynamic pressure decreased as the flight Mach number was increased to 0.8. The data indicate that critical combinations of buffeting and maneuvering tail loads that are above the limit load and approach the design load for the horizontal stabilizer may occur in low-altitude, low-speed flight with rearward center-of-gravity positions at limit design acceleration values.

INTRODUCTION

Airplanes operating at high subsonic Mach numbers have encountered tail buffeting of sufficient magnitude in maneuvering flight to be objectionable to pilots and possibly to endanger the airplane structure. Some previous study has been made of the buffeting problem (see references 1 to 3); however, little of the available data was directly applicable to the estimation of buffeting tail loads for design purposes. A preliminary investigation of buffeting tail loads was accordingly proposed as part of a program of aerodynamic-loads research planned on a high-speed fighter-type airplane. The results of this investigation are presented herein.

Studies have been made to determine the magnitudes and frequencies of the buffeting tail loads at several altitudes for Mach numbers to 0.80. The critical combinations of buffeting and maneuvering tail loads have been ascertained by a comparison with the limit-load and design-load conditions for the horizontal tail.

## SYMBOLS

W	airplane weight, pounds
S	wing area, square feet
n	load factor; airplane normal acceleration at center of gravity (measured perpendicular to thrust line), g units
q	dynamic pressure, pounds per square foot
$S_t$	horizontal-tail area, square feet
M	Mach number
$C_{NA}$	airplane normal-force coefficient ( $nW/qS$ )
$L_t$	balancing tail load, pounds
$\Delta L_{tb}$	incremental tail load due to tail buffeting, pounds
$C_{m0}$	pitching-moment coefficient of wing-fuselage combination at zero lift
$\bar{c}$	mean aerodynamic chord, feet
x	distance from wing-fuselage aerodynamic center to horizontal-tail center of pressure, feet
d	distance from airplane center of gravity to wing-fuselage aerodynamic center, feet

## APPARATUS AND TESTS

## Airplane

The horizontal tail, fuselage, and wing of the high-speed fighter-type airplane used in the investigation were heavily reinforced in order to provide an extra safety margin against failure in the investigation of buffeting loads. A three-view drawing of the test airplane is shown as figure 1; the pertinent characteristics are given in table I.

## Instrumentation

Impact pressure, pressure altitude, and normal acceleration were measured as functions of time with standard NACA recording instruments.

The airspeed head was mounted on a boom extending 1.2 chords ahead of the leading edge of the wing near its right tip, and the NACA airspeed-altitude recorder was located in the right wing to minimize lag effects. The airspeed system was calibrated for position error up to a Mach number of 0.78; this calibration made possible the determination of the flight Mach number to within  $\pm 0.01$ .

Measurements of the shear on the horizontal tail were made by means of wire-resistance strain gages wired in four-arm bridges and attached near the roots of the front and rear spars on both the left and right stabilizers. Strains were recorded as a function of time by a multiple recording oscillograph employing galvanometer elements of 100-cycle-per-second natural frequency damped about 0.6 of critical damping. This combination of damping and frequency ensured approximately linear response for the buffeting frequencies expected. The strain-gage installation was calibrated periodically by applying known loads to the tail of the airplane. The accuracy of the measured buffeting tail-load increment is estimated to be within  $\pm 100$  pounds.

Accelerations at five spanwise locations on the horizontal stabilizer were measured by means of Statham electrical accelerometers. The accelerometers were placed near the chordwise center of twist at semispan stations on the left and right stabilizers of about 0, 38, and 72 inches. The measurements were recorded as a function of time on a multiple recording oscillograph.

#### Tests

All tests were made with the airplane in the clean condition. Normal rated or maximum attainable power was used in 43 of the 49 runs made. Abrupt stalls were made at pressure altitudes of 10,000, 20,000, and 30,000 feet at Mach numbers from 0.21 to 0.63. In these stalls the airplane was pulled up abruptly, the degree of abruptness being limited by the inertia, control power, and stability of the airplane. A series of gradual stalls was also made in turns at 30,000-foot pressure altitude at Mach numbers from 0.33 to 0.65.

For Mach numbers from 0.64 to 0.80, maximum lift coefficients were not reached in the pull-ups. In this speed range, the airplane was pulled up through the buffeting boundary until a prescribed value of acceleration was reached. At this point, recovery from the pull-up was made. Pull-ups in this speed range were made somewhat more slowly than those in the speed range for Mach numbers from 0.21 to 0.65.

#### RESULTS AND DISCUSSION

Three typical load-factor time histories obtained in abrupt pull-ups are shown in figure 2. Point A in each time history represents the

point where buffeting started; point B, the point of peak mean load factor; and point C, the point where buffeting stopped. In figures 2(a) and 2(b) the first two points coincide; whereas in figure 2(c) the peak mean load factor occurs after buffeting starts and between points A and C. The conditions of flight in which buffeting may be encountered have been determined from data of this type.

Typical strain-gage records of buffeting flight are shown in figure 3. The ordinates are the strains at various points in the airplane structure; the abscissas are the time. Points A, B, and C represent the same conditions as in figure 2. Figure 3(a) corresponds to figure 2(a) with points A and B coincident. Figure 3(b) corresponds to figure 2(c) with point B, the peak mean load factor, occurring after the start of buffeting at point A. The buffeting increment in tail load may be defined as the additional value of load superposed on that load required to balance the airplane. This increment is indicated in terms of strain-gage deflection in figure 3(a). The strain at any point in the structure at any time is proportional to the load on the structure at that time. The magnitudes and frequencies of the buffeting tail-load increment have been determined from data similar to those of figure 3.

#### Buffeting Boundaries

Those values of airplane normal-force coefficient corresponding to the beginning of buffeting, or to points A in figure 2, have been plotted in figure 4(a) as a function of Mach number for the pull-ups made in this investigation. The values of normal-force coefficient decrease for Mach numbers increasing from 0.21 to 0.48. The normal-force coefficient then increases to a secondary peak at a Mach number of 0.57 after which it again begins to decrease. As noted previously, in the lower Mach number range the peak mean load factor occurs simultaneously with the start of buffeting; that is, points A and B are coincident. (See fig. 2.) This peak mean load factor corresponds to the maximum airplane normal-force coefficient for the maneuver. The secondary peak in the buffeting-boundary curve is characteristic of the variation of the maximum normal-force coefficient with Mach number for low-drag airfoils. Consideration of the characteristics of low-drag airfoils indicates that the secondary peak is caused by the broadening of the upper-surface low-pressure region which offsets the reduction in the negative pressure peak as the Mach number increases. With further Mach number increase, the decrease in the negative pressure peak more than accounts for the broadening upper-surface pressure, and the maximum normal-force coefficient again begins to decrease.

A secondary buffeting boundary corresponding to gradual stalls of the airplane occurred at normal-force coefficients below the maximum values attainable. Data measured in turns of increasing tightness are given in figure 4(b). The trend of these data is the same as that of the maximum normal-force values corresponding to abrupt pull-ups. Other investigations (references 4 and 5) have demonstrated that the maximum

lift coefficient depends on the rate of change of angle of attack. It can thus be inferred that in the lower speed range a family of buffeting boundaries or maximum-normal-force lines exists between the boundary for gradual stalls (corresponding to wind-tunnel measurements) and the boundary for the absolute maximum normal-force coefficients attainable.

At Mach numbers above 0.64, buffeting begins before maximum normal force is reached. (See dashed part of curve in fig. 4(a).) Between the limits defining these two conditions lies a region in which at any point the airplane is subjected to superposed buffeting tail loads. It is noteworthy that the buffeting loads in this higher speed range have a different origin than those in the lower speed range. The buffeting at the lower speeds arises from the turbulent wake behind a completely stalled wing, whereas buffeting at the higher speeds arises from the turbulent wake behind a wing partially stalled as a result of compressibility shock.

Within the limits of the data shown in figure 4(a), altitude and hence Reynolds number have no effect on the maximum normal-force coefficient and the buffeting boundary as determined in abrupt pull-ups. The results of figure 4(a) may therefore be presented in terms of acceleration or load factor as functions of altitude and Mach number. The results of such a conversion have been plotted in figure 5 for pressure altitudes from sea level to 40,000 feet. As seen in figure 5, at a pressure altitude of 40,000 feet the airplane is capable of only the mildest maneuvers and would be subjected to buffeting in level flight at a Mach number of about 0.79.

#### Buffeting Tail Loads

Magnitude of buffeting tail loads.—The magnitudes of the buffeting tail-load increments were determined from time histories, such as are shown in figure 3, by choosing the maximum strain amplitude from each run. The amplitudes were then converted to half-amplitude resultant loads. The positive and/or negative tail-load increments  $\Delta L_{tb}$  so determined were converted to buffeting coefficients by dividing by the dynamic pressure and the tail area. This coefficient was then plotted in figure 6 as a function of Mach number for pressure altitudes of 10,000 and 30,000 feet for both abrupt and gradual maneuvers. This method of presentation was chosen since the primary variables of stall angle of attack and dynamic pressure were indirectly taken into account (reference 1) because the maximum normal-force coefficient, and hence the stall angle of attack, is a unique function of Mach number.

From figure 6, it may be seen that the buffeting load coefficient tends to decrease with Mach number and the scatter of the data appears about the same for the two test altitudes and the two types of maneuvers. Since the scatter cannot be accounted for by inaccuracies in measurement, the scatter is believed to be due to the fact that the unstable wing flow from which buffeting tail loads arise is aperiodic. The trend of the coefficient

to decrease with increasing Mach number as shown in figure 6 is in qualitative agreement with the conclusions of reference 1 since inspection of figure 4 shows that the normal-force coefficient, and thus the stall angle of attack, tends to decrease with increasing Mach number. Of passing interest is the maximum buffeting tail-load increment measured which was  $\pm 2500$  pounds, corresponding to a Mach number of 0.60, a dynamic pressure of 162 pounds per square foot, and a buffeting load coefficient of 0.376.

In order to extrapolate the results beyond the test conditions, an envelope line has been drawn through the upper points of the data. Of the points determining this line, only one was at a test altitude of 10,000 feet. Use of this upper limit of the data as a basis for the estimation of buffeting tail loads at other altitudes is thus considered conservative.

Character of loads.— The results of high-speed wind-tunnel studies indicate that the frequencies in the wake of a wing extend over a wide range of values. Analysis of the buffeting data from the present investigation shows that certain frequencies are selected by the horizontal tail from the frequencies available. Average values of these frequencies which appear more or less concurrently throughout the speed range of the investigation are listed in table II together with the natural frequencies of the pertinent components of the test airplane as measured by vibration tests. It will be noted that the four lower frequencies found in the tests are approximately equal to the four lower natural frequencies of the airplane structure (that is, fuselage torsion, wing bending, horizontal-tail symmetrical bending). The relationship between buffeting-load frequencies as measured and the natural frequencies of various airplane components has also been established in a comparable Mach number range for a research-type airplane. The greater load amplitudes were found to be associated with the three lower frequencies. Amplitudes of the other frequencies appearing were secondary. With normal rated power, 25 out of 28 cases examined indicated that the buffeting loads of greatest amplitude on the tail plane were out of phase from left to right sides. For throttled engine operation, the loads were in phase from left to right sides in four out of six cases examined. This fact indicates that engine operation is instrumental in causing the flow to separate on one side of the wing before it separates on the other. Qualitatively the reaction of the tail-fuselage combination to the disturbed flow from the wing depends on the way in which the flow breaks down. If the flow breaks from both wings simultaneously, or almost so, the tail may vibrate symmetrically or a few degrees out of phase at its own natural frequency in symmetrical bending. If, however, the flow breaks first from one wing and then the other, the empennage should react at its lowest asymmetrical frequency which is, in this case, the first torsional mode of the fuselage-stabilizer combination.

Estimation of aerodynamic loads.— Since the mass distribution of the horizontal tail is known and the acceleration distribution along the span has been measured (see section entitled "Instrumentation") as a function of time, the resultant buffeting tail load may be corrected at any time for the relieving load due to inertia to obtain the aerodynamic buffeting tail load. Incremental aerodynamic buffeting tail loads have been calculated by this method for a limited number of runs and are shown in figure 7 as a function of the incremental resultant buffeting tail loads. The results are for either left or right side as indicated. The data include points with power off and power on and at two different altitudes. The results indicate that the inertia of the tail plane relieves the aerodynamic buffeting increment by about 35 percent. It should be noted that the results are based on inertia loads calculated for frequencies lower than 25 cycles per second. The relieving effects due to the higher frequencies cannot be estimated accurately although they are believed to be secondary.

Comparison of resultant buffeting tail loads with limit tail load.— The maximum resultant buffeting tail-load increment measured of  $\pm 2500$  pounds is less than half the limit load of 5570 pounds (that load at which the structure yields) of the horizontal stabilizer of a standard fighter-type airplane (without the reinforcement added to the test airplane). It is apparent that measured buffeting tail loads alone are not of sufficient magnitude to cause failure; however, combinations of the buffeting tail-load increment and the maneuvering tail load may possibly exist that exceed the limit load.

Resultant buffeting tail-load increments and the maneuvering tail loads for steady curvilinear flight along the buffeting boundary have been plotted in figure 8 for pressure altitudes from sea level to 40,000 feet. The resultant buffeting tail-load increments shown in figure 8(a) have been calculated from the envelope line of figure 6. As was pointed out previously in connection with figure 6, use of this envelope line for extrapolation to other altitudes is considered conservative. The tail loads for steady curvilinear flight shown in figure 8(b) were calculated from the balancing tail-load equation where

$$L_t = -C_{m0} \frac{q}{\sqrt{1 - M^2}} \frac{Sc}{x} + \frac{nWd}{x}$$

The values of  $C_{m0}$  and  $d$  used were estimated from recent results of tail-load measurements on the test airplane at the same center-of-gravity position (25.1 percent M.A.C.); the values of  $n$  were obtained from figure 5. From figure 8, critical conditions are seen to exist at high-speed sea-level flight and at medium-speed sea-level flight. Inherent in the design of any airplane are certain physical limitations which the pilot must observe. The first of these limitations is a value of normal acceleration beyond which the pilot must not pass. For this

test airplane with its take-off weight, the limit is  $7.22g$ . A line indicating this limit is drawn in both figures 8(a) and 8(b). A second limitation is one of maximum permissible diving speed. For this airplane, the true permissible diving speed is 537 miles per hour. This limit is also indicated in figures 8(a) and 8(b). The crosshatched area represents operation beyond these two limits. The assumption that the pilot stays within airplane restrictions alters the situation considerably, inasmuch as the most critical condition is now at sea level at a Mach number of 0.37 where the maximum sum of the two components is 6800 pounds which is above the limit load of 5570 pounds. With this conservative method of extrapolation, combinations of the resultant buffeting tail-load increment and the maneuvering tail load that are greater than the limit stabilizer load exist for accelerations within the V-n diagram for altitudes near sea level. Without the relieving effect of the tail inertia, the combination at a Mach number of 0.37 produces an aerodynamic load of about 9400 pounds. Moving the center of gravity to its maximum allowable rearward position of about 32 percent mean aerodynamic chord adds about 1700 pounds to the total tail load at a load factor of  $7.22g$ . This addition to the combination of resultant buffeting and maneuvering tail loads would raise the critical combination to about 8500 pounds which is above the design or failure load of the horizontal stabilizer. Values of the combination of buffeting tail load and maneuvering tail load that are greater than the limit load exist for operation at  $7.22g$  with the center of gravity at 32 percent mean aerodynamic chord for all altitudes below about 22,000 feet. It is apparent then that, based on this conservative extrapolation of the test results, the critical combination of the buffeting tail-load increment and maneuvering tail load occurs at sea level at the lowest speed at which the limit design acceleration can be attained — the center of gravity being located at its maximum rearward position — and that this load is of sufficient magnitude to cause failure of the horizontal stabilizer.

#### SUMMARY OF RESULTS

Pertinent results of the buffeting investigation which apply to the test airplane are summarized as follows:

At Mach numbers below about 0.64, buffeting of the horizontal tail occurred simultaneously with the attainment of maximum normal force. At higher Mach numbers, buffeting occurred before the attainment of maximum normal force. Reynolds number had no appreciable effect on the maximum normal-force coefficients and, hence, the buffeting boundary determined in abrupt pull-ups.

The magnitude of maximum buffeting tail loads for unit dynamic-pressure values decreased with increasing Mach number. The magnitude of the buffeting increment itself was not sufficiently great to cause failure. The relieving effect due to inertia of the tail plane reduced the aerodynamic buffeting tail-load increment about 35 percent.

Buffeting frequencies selected by the horizontal tail from the range of frequencies existing in the disturbed wing flow corresponded to basic frequencies of the airplane structure. The buffeting loads were both symmetrical and asymmetrical, the buffeting loads being predominantly asymmetrical in character during powered flight.

Critical combinations of buffeting and maneuvering tail loads that are above the limit load and approach the design load for the horizontal stabilizer may occur in low-altitude, low-speed flight with rearward center-of-gravity positions at limit design acceleration values.

#### CONCLUDING REMARKS

Further study of the buffeting phenomenon, including tests to determine the effect of altitude and structural frequencies on the magnitude of buffeting tail loads, is necessary; however, until these effects have been determined, the following general trends are believed to be applicable to airplanes having a conventional (tail behind wing) configuration:

The magnitude of maximum buffeting tail loads for constant dynamic-pressure values may be expected to decrease with increasing Mach number, at least to a Mach number of 0.8. The critical combinations of buffeting and maneuvering tail loads will probably occur at low operating altitudes at the lowest speed at which the limit design acceleration can be attained, the center of gravity being located at its maximum rearward position.

The buffeting frequencies selected by the horizontal tail from the range of frequencies existing in the disturbed wing flow may be expected to correspond to basic frequencies of the airplane structure. The buffeting loads may act either symmetrically or asymmetrically depending on the way in which the disturbed flow originates.

Langley Aeronautical Laboratory  
National Advisory Committee for Aeronautics  
Langley Field, Va., June 4, 1948

## REFERENCES

1. Abd rashitov, G.: Tail Buffeting. NACA TM No. 1041, 1943.
2. Boshar, John: Some Flight Measurements of Pressure Distribution during Tail Buffeting. NACA MR No. L5J06, 1945.
3. Flight Research Maneuvers Section: Flight Studies of the Horizontal-Tail Loads Experienced by a Fighter Airplane in Abrupt Maneuvers. NACA Rep. No. 792, 1944.
4. Kramer, Max: Increase in the Maximum Lift of an Airplane Wing Due to a Sudden Increase in Its Effective Angle of Attack Resulting from a Gust. NACA TM No. 678, 1932.
5. Farren, W. S.: The Reaction on a Wing Whose Angle of Incidence Is Changing Rapidly. Wind Tunnel Experiments with a Short Period Recording Balance. R. & M. No. 1648, British A.R.C., 1935.

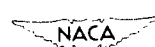
TABLE I  
CHARACTERISTICS OF AIRPLANE

Wing:	
Span, ft . . . . .	37.03
Area, sq ft . . . . .	240.1
Mean aerodynamic chord, ft . . . . .	6.63
Airfoil . . . . .	Low drag
Horizontal tail:	
Span, ft . . . . .	13.18
Area, sq ft . . . . .	41.0
Incidence, deg . . . . .	1
Weight at take-off, lb . . . . .	8850
Center-of-gravity position (at take-off), percent M.A.C. . . . .	25.1



TABLE II  
FREQUENCY CHARACTERISTICS

Buffeting frequencies (determined from strain-gage measurements on horizontal tail), cps . . . . .	9, 11, 23, 70, 130
Natural frequencies, cps	
Wing:	
Primary bending . . . . .	11.9
Asymmetric bending . . . . .	22.3
Primary torsion . . . . .	37.4
Horizontal tail:	
Primary bending . . . . .	23.6
Asymmetric bending . . . . .	67.9
Torsion . . . . .	>70
Fuselage:	
Torsion . . . . .	9.8
Bending (side) . . . . .	13.6



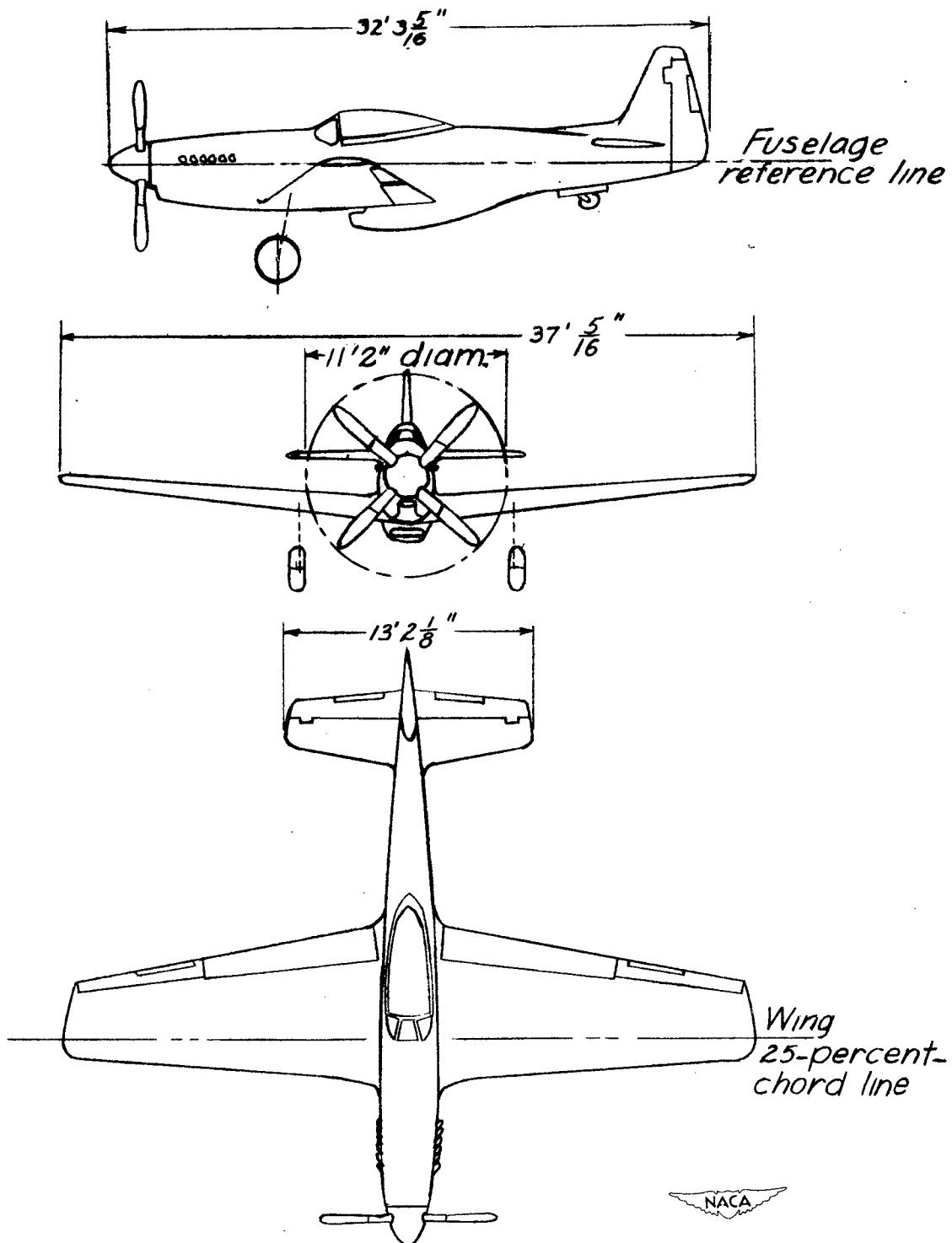


Figure 1.- Three-view diagram of test airplane.

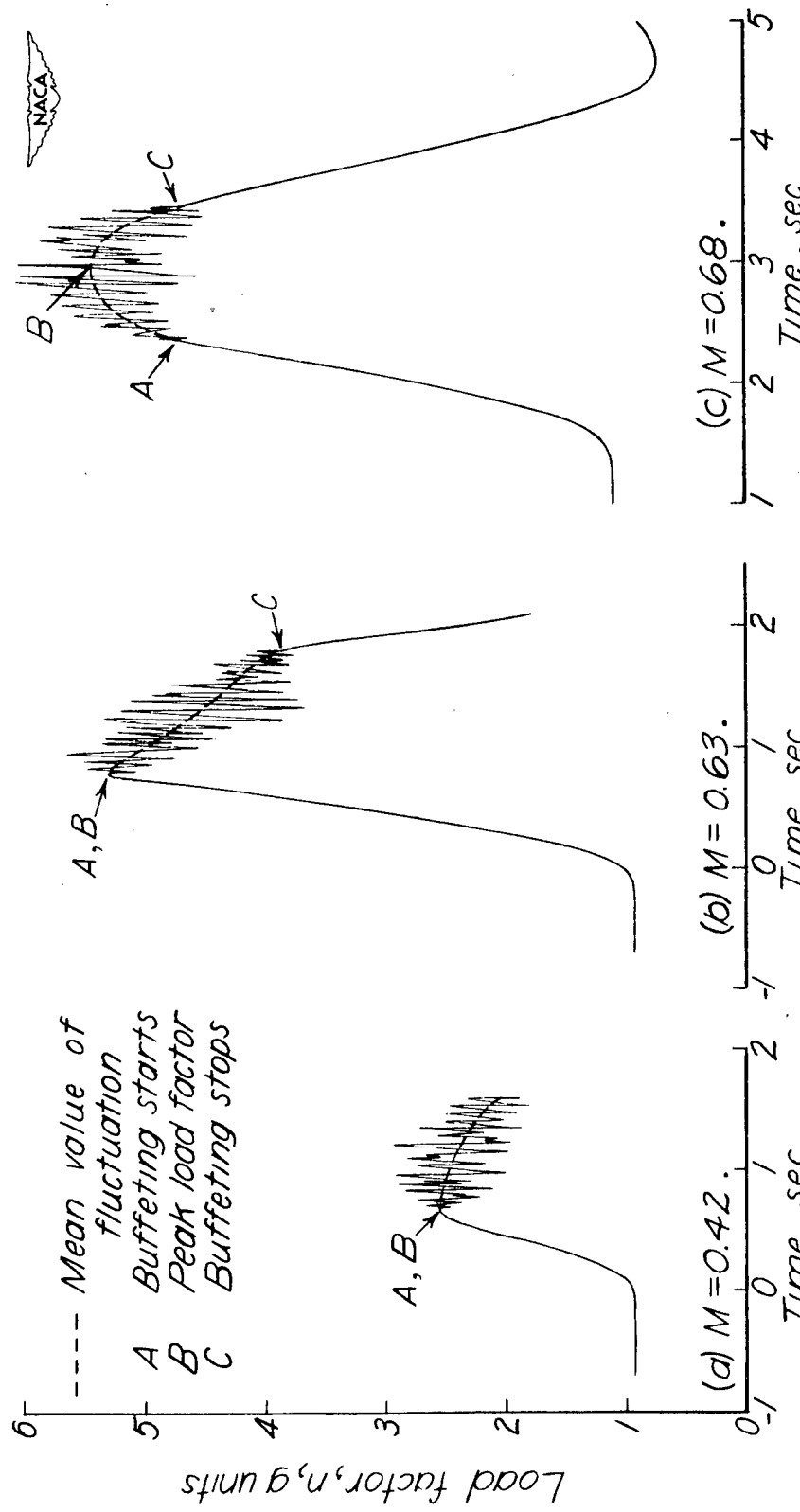
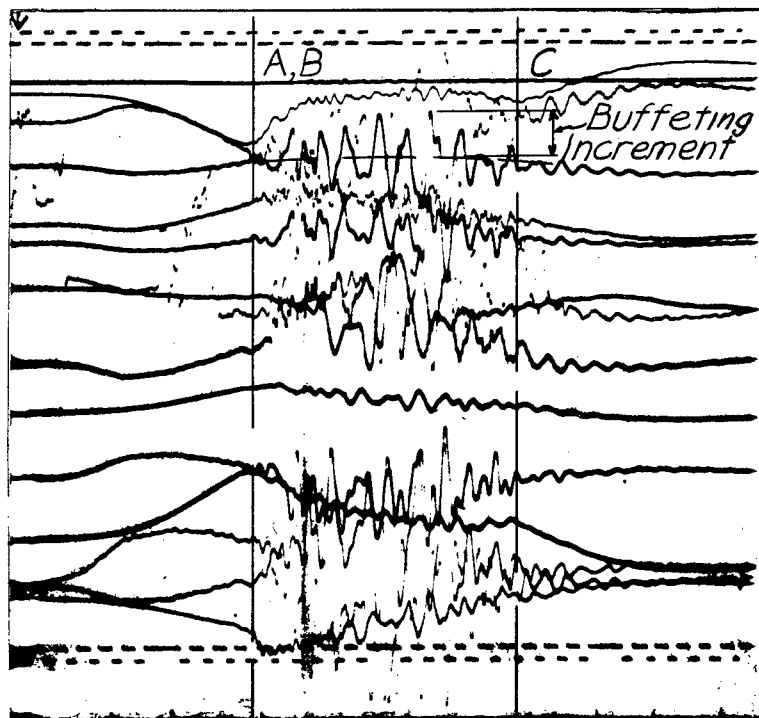
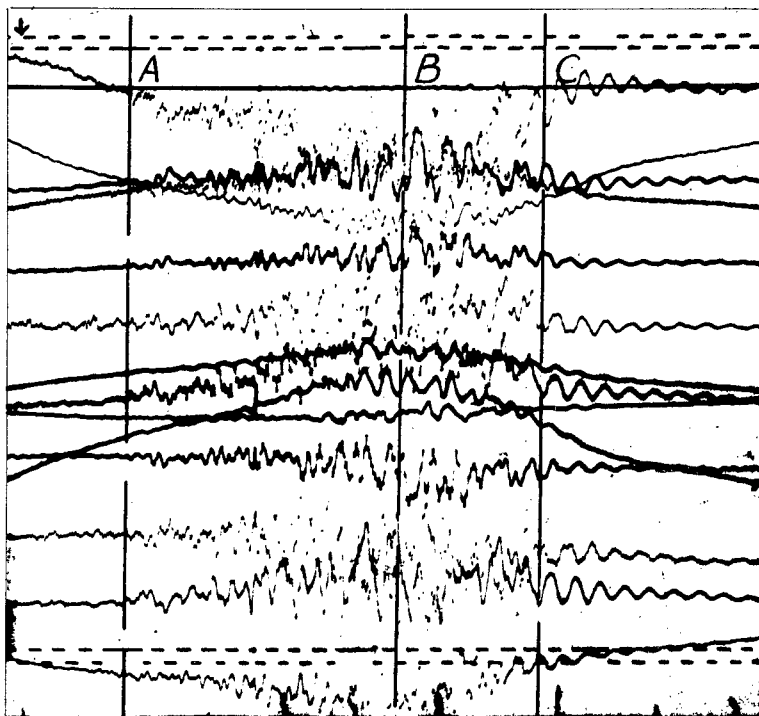


Figure 2.-Typical time histories of normal load factors in abrupt pull-ups at an altitude of 30,000 feet.



(a)  $M = 0.25$ ; pressure altitude, 10,000 feet.



(b)  $M = 0.70$ ; pressure altitude, 30,000 feet.



Figure 3.— Typical strain-gage records in abrupt pull-ups.

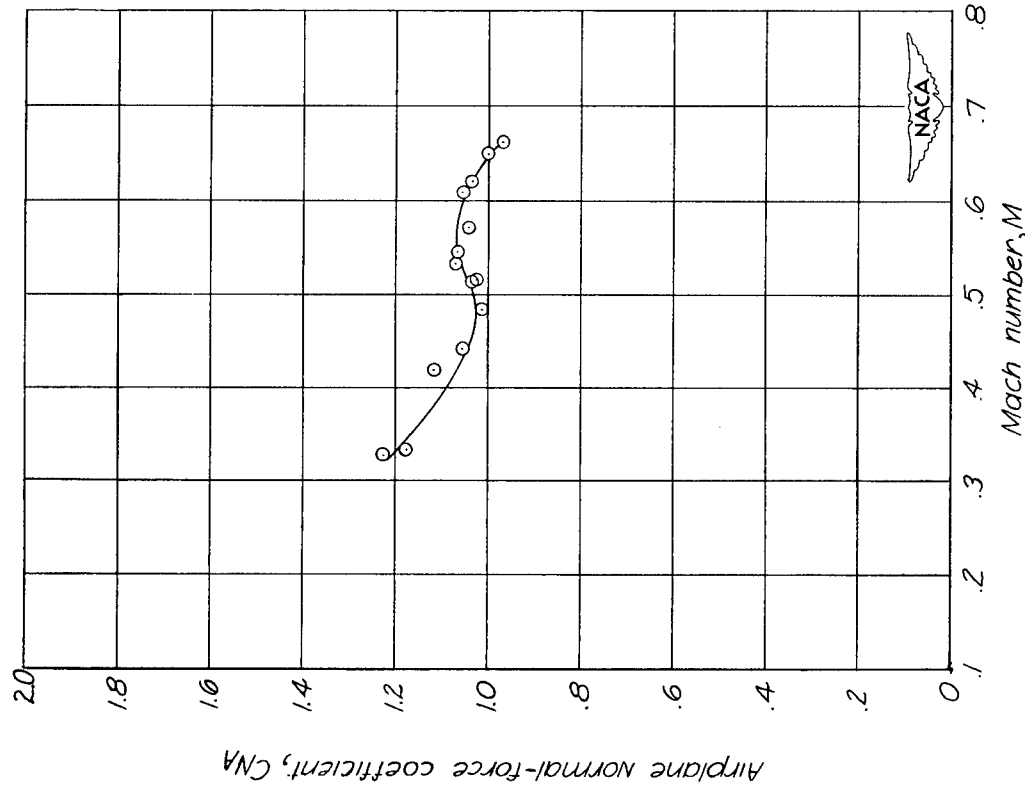
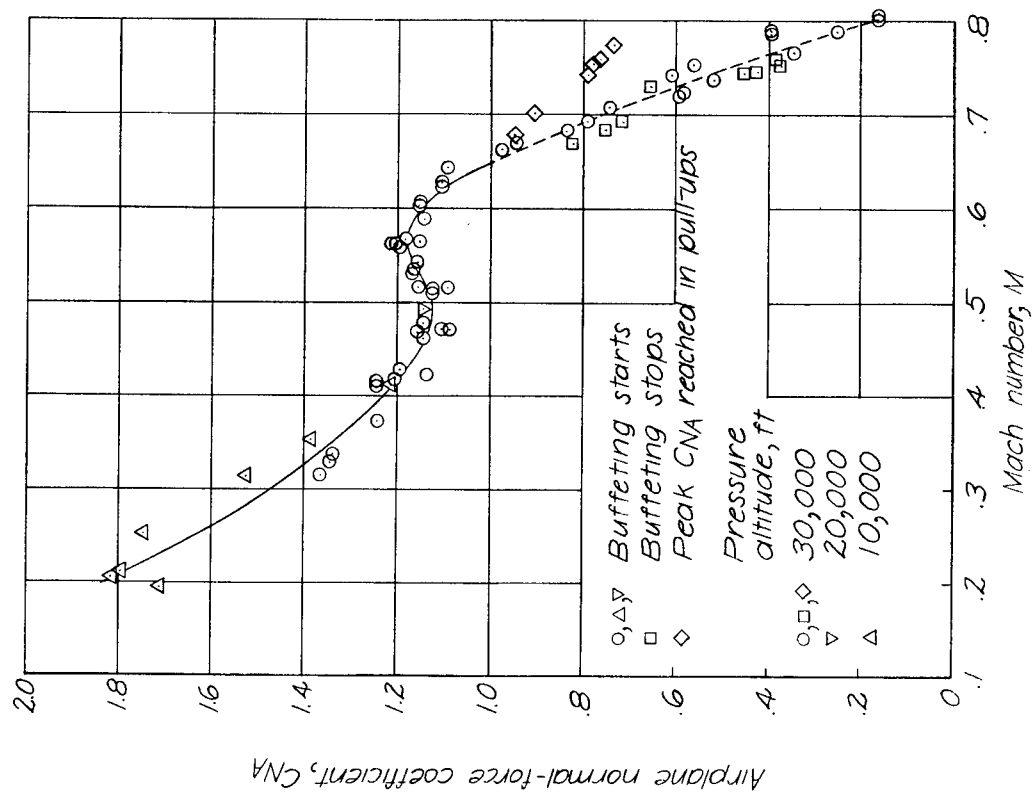


Figure 4.- Buffeting boundaries obtained in abrupt and gradual stalls for test airplane.  
 (a) Abrupt pull-ups.  
 (b) Gradual stalls in turns.



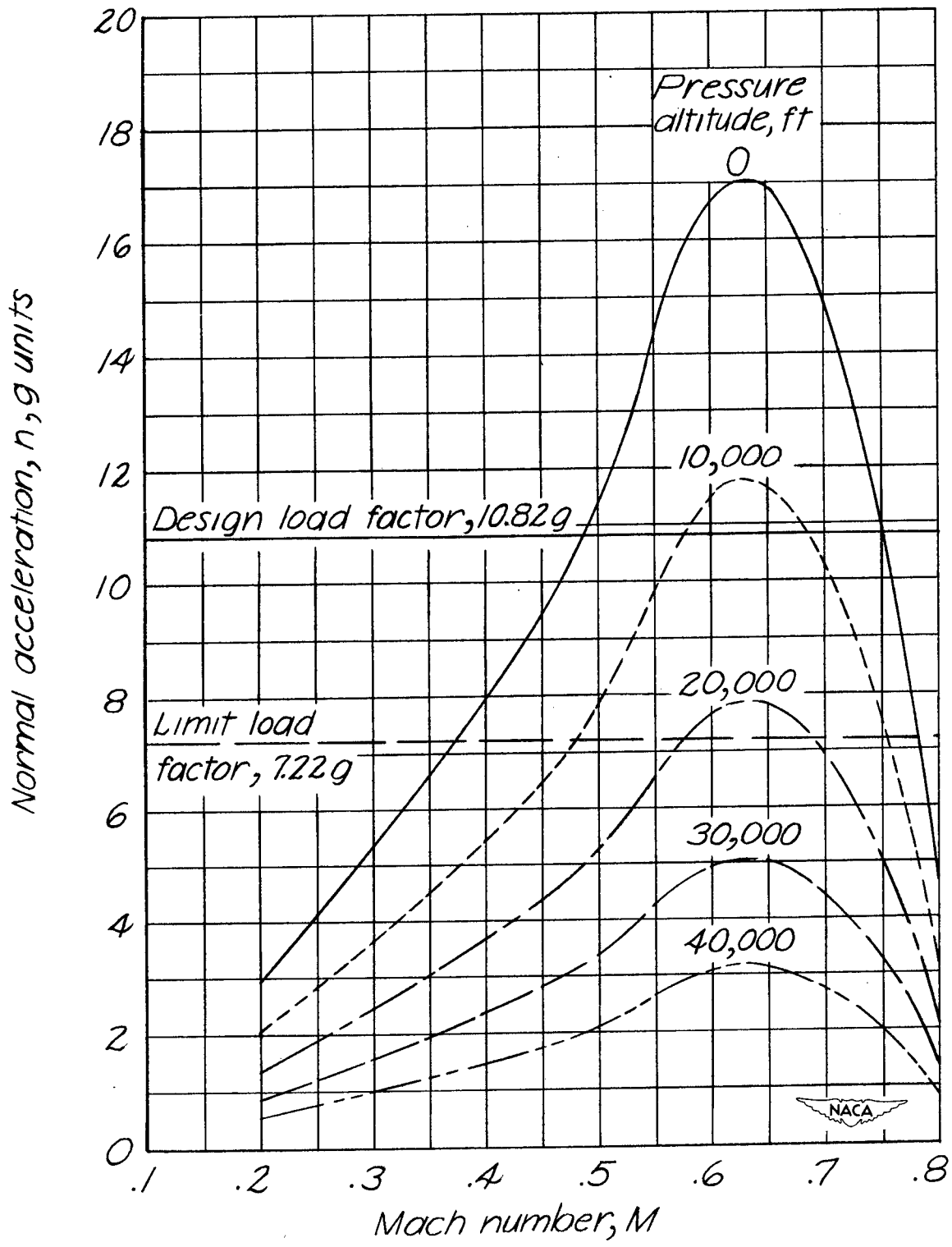


Figure 5.—Buffeting boundaries at various altitudes  
for test airplane.

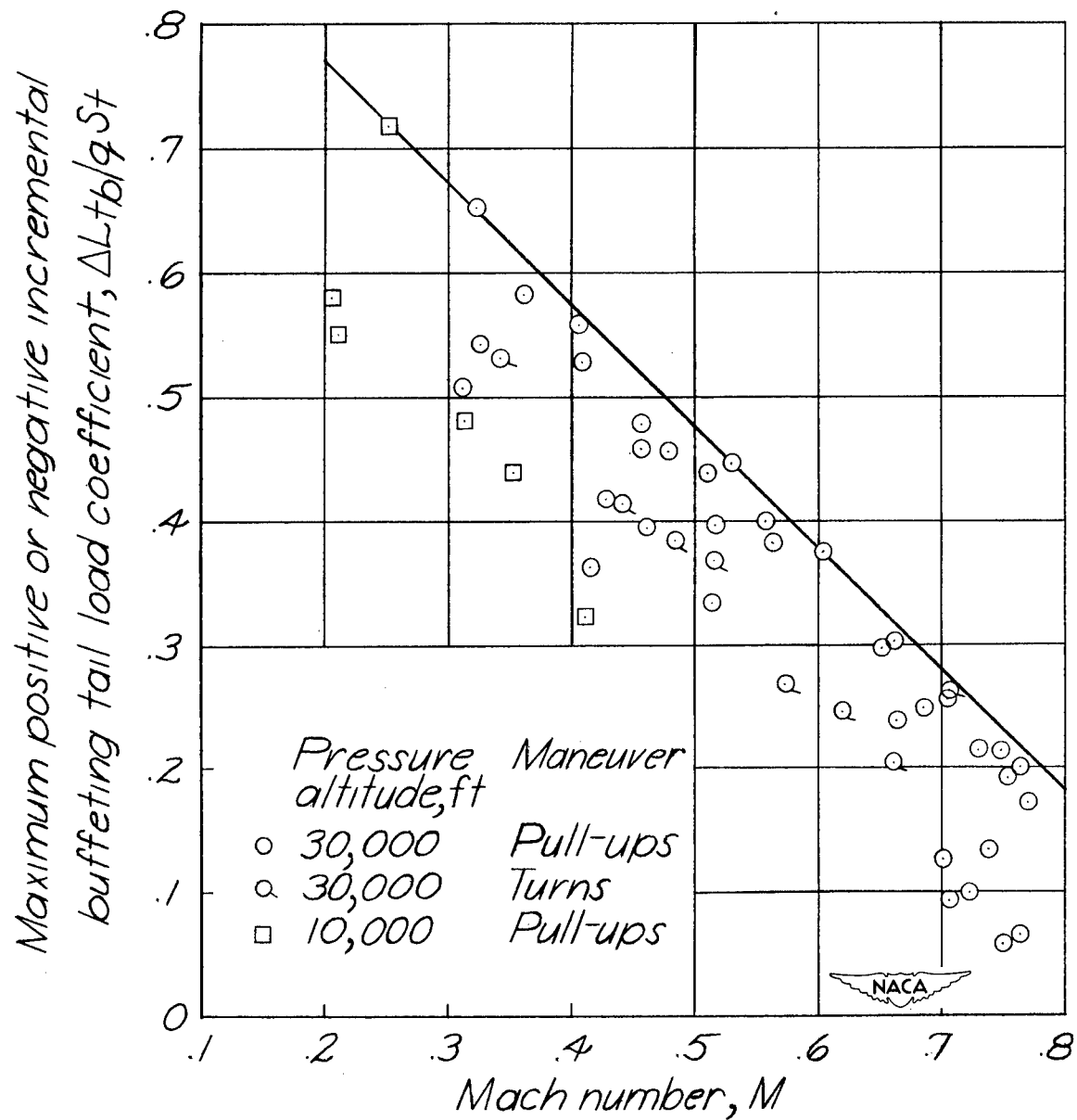


Figure 6.—Maximum incremental buffeting tail load coefficient as a function of Mach number for test airplane.

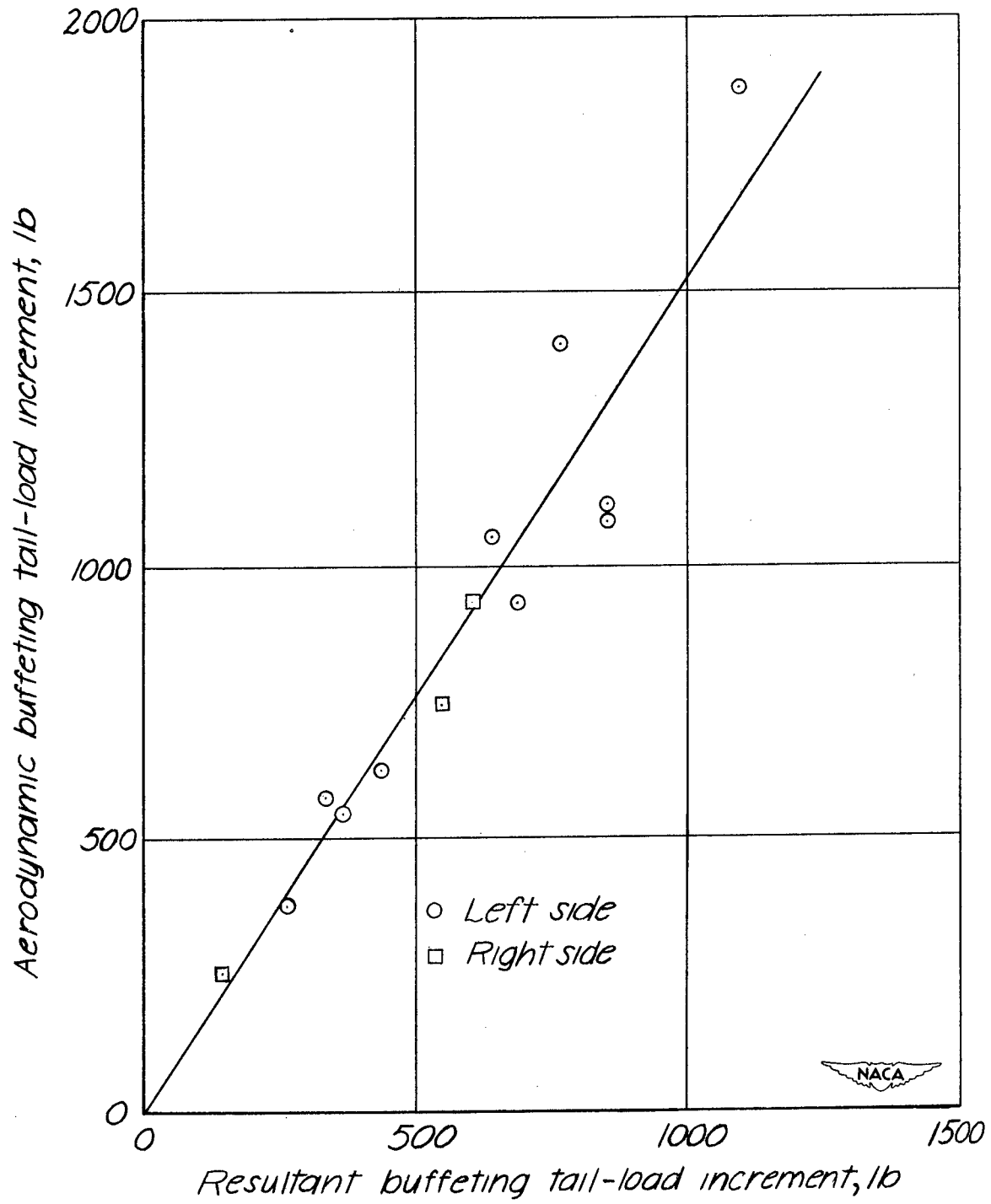


Figure 7.—Comparison of aerodynamic and resultant buffeting tail-load increments for test airplane.

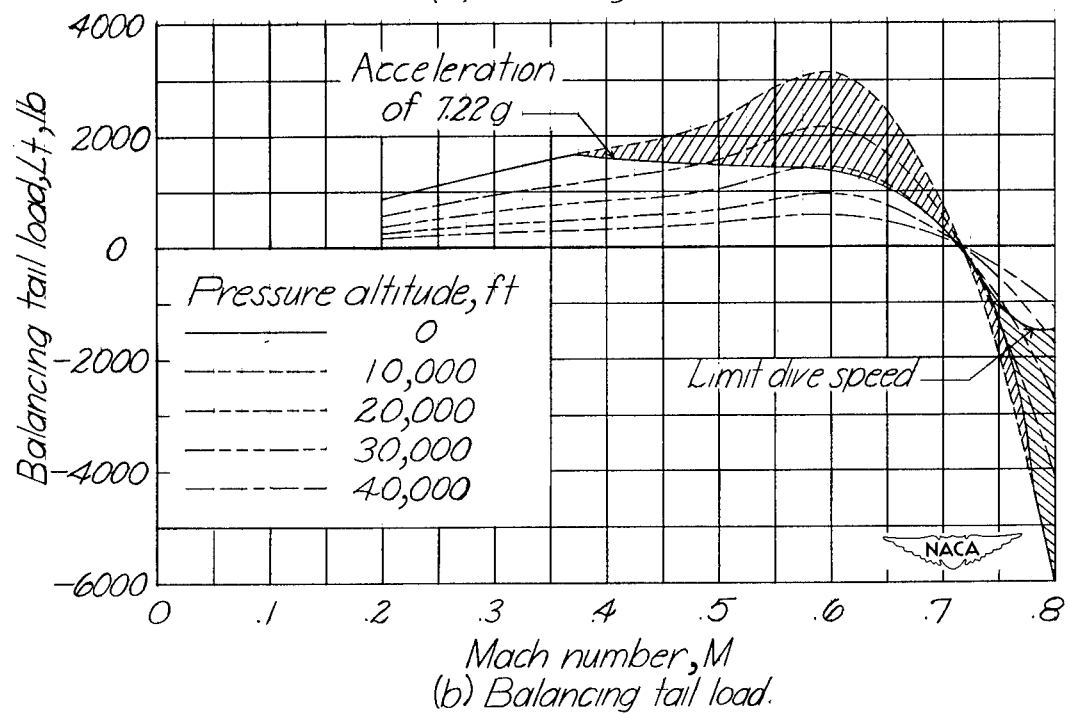
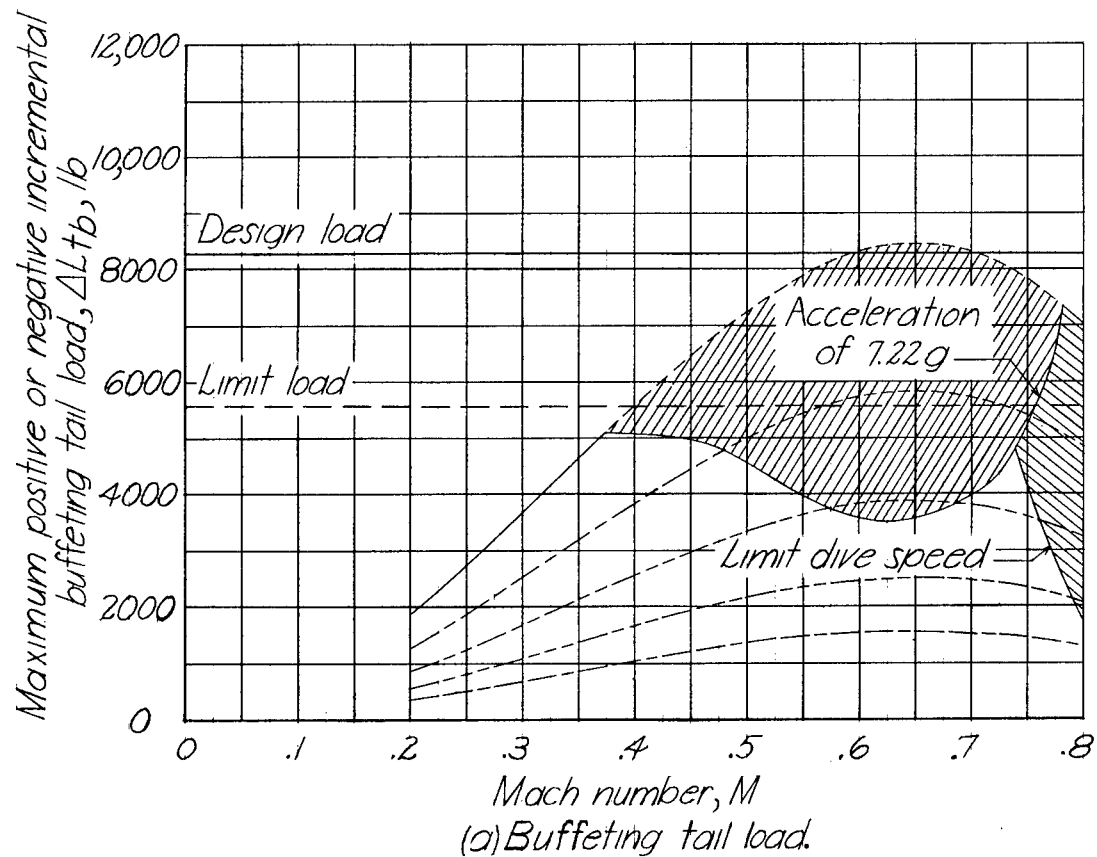


Figure 8.—Estimated buffeting tail-load increments and maneuvering tail loads along buffeting boundaries for several altitudes.